ELSEVIER

Journal of Hydrology 272 (2003) 203–212

Journal of Hydrology

www.elsevier.com/locate/jhydrol

Measurement of sated hydraulic conductivity of surface soil in the field with a small-plot sprinkling infiltrometer

K.A. Suleiman[a], D. Swartzendruber[b,*]

[a]*Faculty of Agriculture, Al-Fatah University, Tripoli, Libya*
[b]*Department of Agronomy and Horticulture, University of Nebraska-Lincoln, 246 Keim Hall, Lincoln, NE 68583 0915, USA*

Abstract

The purpose of this study was to determine the sated (near-saturated) hydraulic conductivity, K, of surface soil in the field. With K as a parameter, an equation describing cumulative water runoff from a small-plot sprinkling infiltrometer was developed from an empirical infiltration equation matched to Green–Ampt infiltration theory for constant-intensity water application; also incorporated was a fixed-average static concept of surface water storage on the small soil plot. To evaluate K, this runoff equation was fitted by least squares to field data from a small-plot (1.16 m × 1.16 m) sprinkling infiltrometer on four combinations of soil type and cover: Clermont and Cincinnati silt loam (grass), and Chelsea sandy loam (grass and fiberglass). The runoff equation fitted the field data very well, especially at times greater than 10–15 min after the first appearance of water runoff. The order of the mean K values for the four soils-cover combinations was: Chelsea-grass > Chelsea-fiberglass > Cincinnati-grass > Clermont-grass, which is compatible with the physical characteristics of these soils and covers. Of the various differences between mean K values, half were statistically significant. The fixed-average static surface-water storage behaved in reasonable fashion, both physically and statistically, and in regard to site slope and plot cover.

Keywords: Hydraulic conductivity; Infiltrometer; Green–Ampt model; Infiltration

1. Introduction

The saturated hydraulic conductivity K_s of a soil is arguably the single most important and significant point on the curve of hydraulic conductivity versus soil water content. Over the range in water content from saturation (all soil pores completely filled with water) to dryness, K_s is not only the maximum conductivity but is also of direct utility in its own right as it relates to such matters as soil drainage, the disposal of liquid waste on land, and soil classification. Ironically, however, in almost all considerations and discussions of K_s, the actual water condition is seldom that of saturation. If special measures are not taken during the wetting of soil with water, such as removing the soil air by vacuum or displacing it with water-soluble gas, or subjecting the wetted soil to prolonged water flow, then true saturation will not be realized. In the common but superficial way of attempting to attain water saturation, by bringing free water in contact with soil while both are at atmospheric pressure, the resulting water content on a volumetric basis can range from 75% for fine-textured soil to 95% for coarse-textured soil. The corresponding unfilled porosity, ranging from 25 to 5%, will contain entrapped air and hence is not

* Corresponding author. Tel.: +1-402-472-1568; fax: +1-402-472-7904.
E-mail address: agrohort@unl.edu (D. Swartzendruber).

0022-1694/03/$ - see front matter © 2002 Elsevier Science B.V. All rights reserved.
PII: S0022-1694(02)00265-2

accessible for the flow of water. To denote this near-saturated (though still unsaturated) condition due to entrapped air, Miller and Bresler (1977) introduced the term 'satiated' to distinguish it from the truly saturated case. A dictionary synonym is the shorter term 'sated', which we shall use here and symbolize as K.

The measurement of K in the field has proved to be difficult, especially for the surface-zone region in which a water table seldom or never occurs. A possible approach is to employ the small sprinkling infiltrometer that applies water at a constant rate to a plot on the order of 1 m × 1 m in size (Bertrand and Parr, 1961a,b; Amerman et al., 1970; Rawitz et al., 1972). Also, the generally good reproducibility of this type of instrument was a further motivation for utilizing it to measure K. Therefore, the purposes of this study were (i) to develop an appropriate theoretical approach for determining K from the cumulative water runoff from a small sprinkling infiltrometer field plot, and (ii) to test the approach experimentally on several different soils, covers, and initial soil moisture, by using existing data originally obtained primarily for measuring water infiltration in the field.

2. Theory for small-plot water runoff

Employing rectangularly shaped water-content profiles, as first introduced in the classic approach of Green and Ampt (1911) for water infiltration from a layer of free water ponded on the soil surface, Swartzendruber (1974) derived the mathematical solution for water infiltration from constant-intensity water application to a soil surface. Because these resulting constant-intensity Green–Ampt equations, for rate or quantity of infiltrated water, were not explicit with time, he then introduced the alternative, time-explicit equation

$$i = B(t - c)^{-1/2} + K \tag{1}$$

where i is the one-dimensional downward volumetric water-infiltration flux (volume of water per unit of bulk soil cross-sectional area per unit time), B and c are constants for a given fixed water application intensity r, and t is the time after starting and maintaining the constant intensity r. It was found that an integrated form of Eq. (1) could be matched with its counterpart constant-intensity Green–Ampt equation within an error of ± 11% over the complete r range of $K \leq r \leq \infty$.

The matching process also specified a relationship between the dimensionless quantities c/t_0 and K/r, with $t = t_0$ being the time required for the first and infinitesimally thin film of free water to appear on the soil surface. Expressing c/t_0 in the alternative form

$$C = (t_0 - c)/t_0 \tag{2}$$

numerical values of C versus K/r were provided (Swartzendruber, 1974). We have here employed these values to prepare the dimensionless graph in Fig. 1.

To develop a runoff equation that contains K, we begin by considering Eq. (1) to be applicable only for the time range $t \geq t_0$. Prior to and at t_0, for $0 \leq t \leq t_0$, the infiltration flux at the soil surface is simply equal to r, meaning that all of the sprinkling-applied water is infiltrated into the soil without accumulating on the soil surface or running off. Hence, we have $i = r$ at $t = t_0$. Putting this condition into Eq. (1) evaluates B as $B = (r - K)(t_0 - c)^{1/2}$, which if substituted back

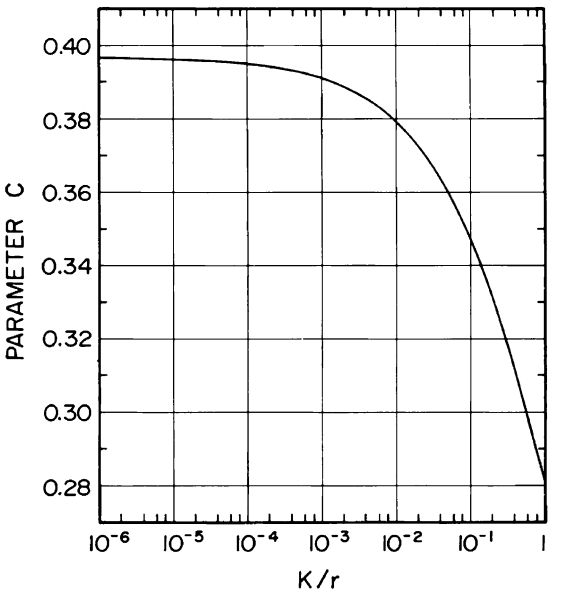

Fig. 1. Parameter C of Eq. (2) as a function of K/r, graphed from the data of Swartzendruber (1974).

into Eq. (1) yields

$$i = (r - K)[(t_0 - c)/(t - c)]^{1/2} + K \quad (3)$$

For $t \geq t_0$, the rate of formation of free surface water excess is $dz/dt = r - i$, where z is the cumulative free surface water excess expressed as a depth (volume of water per unit bulk area of soil surface). Using Eq. (3) to express i in $dz/dt = r - i$ then gives

$$dz/dt = (r - K)\{1 - [(t_0 - c)/(t - c)]^{1/2}\} \quad (4)$$

Separating variables in Eq. (4), integrating, and using the condition $z = 0$ at $t = t_0$ to evaluate the constant of integration, we get, after rearranging and simplifying

$$z = (r - K)[(t - c)^{1/2} - (t_0 - c)^{1/2}]^2 \quad (5)$$

For water application on a relatively small soil area (on the order of 1 m × 1 m), we introduce a highly simplified approximate model of free water storage on the soil surface. Using $z = z_1$ at $t = t_1$ in Eq. (5), where $t_1 > t_0$, we obtain

$$z_1 = (r - K)[(t_1 - c)^{1/2} - (t_0 - c)^{1/2}]^2 \quad (6)$$

Once $z = z_1$, we assume that all subsequently applied water excess becomes runoff rather than causing the stored-water depth to exceed z_1. Therefore, we take the cumulative water runoff to be $w = z - z_1$, which from Eqs. (5) and (6) becomes

$$w = (r - K)\{t - 2(t_0 - c)^{1/2}(t - c)^{1/2} - [t_1 - 2(t_0 - c)^{1/2}(t_1 - c)^{1/2}]\} \quad (7)$$

Lastly, to link Eq. (7) with the constant-intensity Green–Ampt model by means of the graph in Fig. 1, as already mentioned in connection with Eq. (2), we substitute Eq. (2) into Eq. (7) to obtain

$$w = (r - K)\{t - 2(Ct_0)^{1/2}[t - (1 - C)t_0]^{1/2} - t_1 + 2(Ct_0)^{1/2}[t_1 - (1 - C)t_0]^{1/2}\}. \quad (8)$$

3. Experimental methods

3.1. Field instrumentation and measurements

The field infiltration measurements were made with the Purdue sprinkling infiltrometer (Bertrand and Parr, 1961a,b). Simulated rainfall at constant intensity was applied to a 3 m diameter circular area of soil surface from a nozzle 2.7 m above the ground. At the center of the wetted surface, a square plot 1.16 m × 1.16 m was delimited by a 15 cm high sheet metal frame inserted 10 cm into the soil, the large surrounding wetted area producing essentially one-dimensional downward infiltration within the plot. Water runoff was collected from the lowest surface-edge of the soil plot, and the cumulative runoff versus time, or hydrograph, was recorded continuously. Before and after water application to the soil plot, the application intensity r was measured by placing a special metal pan, also 1.16 m × 1.16 m, over the plot frame and recording the constant runoff intensity for 10 min.

For each plot, the first application of water to measure runoff, at the initially existing soil water content, was called the dry run. One day later, a second water application to measure runoff, called the wet run because the soil was still wet from the previous day, was made on the same plot. For both dry and wet runs, the period of water application on the soil was about 1 h.

3.2. Collection of data

From data already taken with the Purdue infiltrometer but only for soils with surface cover, we chose 32 hydrographs from the experiments of Gilman (1962) conducted near North Vernon, IN, USA, with standing bromegrass cover clipped back to a height of 10–15 cm on all plots. At a site slope of 0.5% on Clermont silt loam (Typic Ochraqualf fine silty, mixed, mesic; 13% sand, 73% silt, and 14% clay), there were 14 hydrographs. At a site slope of 5% on Cincinnati silt loam (Typic Fragiudalf fine silty, mixed, mesic; 5% sand, 76% silt, and 19% clay), there were 18 hydrographs. From the experiments of Lambert (1970), conducted near West Lafayette, IN, USA, we chose 12 tipping-bucket hydrographs. At a site slope of essentially zero on Chelsea sandy loam (Alfic Udipsamment sandy, mixed, mesic; 59% sand, 40% silt, and 1% clay), there were 8 hydrographs for the 10–15 cm alfalfa-bromegrass cover. On the other 4 plots, 2.5 cm of the uppermost sod surface was removed and then covered with four layers of spun fiberglass.

3.3. Statistical analysis

There were, unfortunately, no separate, independent measurements of K for the soils and conditions here studied, to enable a direct comparison of K values by two methods. Statistical analyses, therefore, were carried out to assess the capability of K, and also of the static surface storage z_1, for detecting differences between soils and cover conditions and to relate K and z_1 behavior to other physical expectations. We used the split plot design for analysis of variance, with the main effects being soils and cover, and the split being between dry and wet runs. Since all main effects and many interactions were statistically significant at the 5% level, least significant differences (LSD) were calculated for dry versus wet comparisons within each soil and cover, while Duncan's multiple range test for unequal groups was employed to compare soils and cover within wet or dry.

3.4. Equation fitting

To apply Eq. (8) to the experimental data of cumulative runoff versus time, we define a transformed (but not dimensionless) time T by

$$T = t - 2(Ct_0)^{1/2}[t - (1 - C)t_0]^{1/2} \tag{9}$$

If $T = T_1$ when $t = t_1$, then

$$T_1 = t_1 - 2(Ct_0)^{1/2}[t_1 - (1 - C)t_0]^{1/2} \tag{10}$$

which by the standard quadratic formula is solved for t_1 to obtain

$$t_1 = T_1 + 2Ct_0 \pm 2[Ct_0(T_1 + 2Ct_0 - t_0)]^{1/2} \tag{11}$$

In terms of Eqs. (9) and (10), Eq. (8) then takes the linear form

$$w = (r - K)(T - T_1) \tag{12}$$

To fit Eq. (12) to runoff data, trial values of C and t_0 are used to calculate T from the experimental time values using Eq. (9). For first estimates, use the approximate midpoint of the C range, $C = 0.34$; for t_0, a plot of experimental cumulative runoff versus time can be projected back to when the runoff curve appears to intersect the time axis. A plot of w versus T assesses the degree to which the linearity of Eq. (12) has been achieved, as evaluated by a minimized residual sum of squares for a linear regression of w versus T. Calculating K from the resulting value of $(r - K)$ and the known r, the ratio K/r is then computed, and from it the corresponding C is determined from Fig. 1. If this C does not agree with the trial C, a new trial C is selected and the foregoing process repeated until there is agreement between the two values of C. With t_0, C, $(r - K)$, K, and T_1 thus evaluated, t_1 is calculated from Eq. (11), and z_1 from Eq. (6) but wherein $(1 - C)t_0$ replaces c, in accordance with Eq. (2) as solved for c.

In some data sets, the foregoing fitting procedure produced $t_1 < t_0$, which of course is impossible physically because runoff cannot occur prior to the beginning of free surface water excess. For these data sets, therefore, we set t_1 equal to its smallest possible physical limit, $t_1 = t_0$, which in turn forces $z_1 = 0$ from Eq. (6) and causes Eq. (8) to become

$$w = (r - K)\{t - 2(Ct_0)^{1/2}[t - (1 - C)t_0]^{1/2} - t_0(1 - 2C)\} \tag{13}$$

Defining a new transformed time U by

$$U = t - 2(Ct_0)^{1/2}[t - (1 - C)t_0]^{1/2} - t_0(1 - 2C) \tag{14}$$

enables Eq. (13) to be written

$$w = (r - K)U \tag{15}$$

Trial values of C and t_0 were then used in Eq. (14) to calculate U from t, just as done previously in Eq. (9) to calculate T from t. In determining the linear regression of experimental w versus U, however, one must use the least-squares formula which forces the linear regression line through the origin, in accordance with Eq. (15).

In a few instances, the square root in Eq. (9) or (14) produced an imaginary value if the first experimental t value was somehow too small. This occasional occurrence was handled simply by deleting the first (w, t) pair from the experimental set of $w(t)$.

4. Results

4.1. Goodness of fit of runoff equations

All fitted parameters and some related numerical values for the three soils are given individually in

Table 1
Fitted parameters of Eq. (8), (13), or (6), and related data for Cincinnati silt loam in the field under grass cover

Plot no.	Initial moisture	K (cm/h)	t_0 (min)	t_1 (min)	C	z_1 (mm)	Residual mean square (10^{-2} mm^2)	r (cm/h)
1	Dry	1.54	3.348	6.103	0.3360	1.07	5.66	9.3276
	Wet	2.00	4.146	4.146	0.3280	0.00	11.61	8.8722
2	Dry	2.26	3.399	6.382	0.3262	1.11	6.15	9.3276
	Wet	2.53	3.191	3.857	0.3216	0.09	3.02	8.8722
3	Dry	2.45	3.771	3.771	0.3216	0.00	1.37	8.6034
	Wet	2.47	3.021	3.021	0.3208	0.00	4.41	8.5050
4	Dry	1.88	2.882	4.796	0.3300	0.61	2.14	9.0228
	Wet	1.32	1.977	3.843	0.3372	0.71	6.60	8.4408
5	Dry	1.39	3.566	4.674	0.3376	0.23	4.07	9.0228
	Wet	1.63	2.414	4.924	0.3320	0.97	5.62	8.4408
6	Dry	4.16	5.672	6.490	0.3080	0.07	10.51	9.3276
	Wet	2.16	6.170	6.170	0.3246	0.00	48.25	8.4408
7	Dry	2.49	4.431	4.431	0.3200	0.00	10.70	8.2782
	Wet	1.90	2.383	2.383	0.3262	0.00	5.89	7.8366
8	Dry	2.75	5.108	5.108	0.3170	0.00	12.66	8.2782
	Wet	1.86	3.175	3.838	0.3268	0.08	4.60	7.8366
9	Dry	1.40	6.588	6.588	0.3368	0.00	13.14	8.6034
	Wet	1.13	2.689	4.786	0.3392	0.68	2.86	7.8366
Mean	Dry	2.26	–	–	–	0.34	–	–
Mean	Wet	1.89	–	–	–	0.28	–	–

Tables 1, 2, and 3. Then, to determine how well Eqs. (8) and (12) or (13) and (15) would describe the experimental runoff data graphically, we selected from each soil the plot that produced the data set with the largest residual mean square (RMS) and hence the poorest fit for that soil. We begin with the largest RMS, 0.4825 mm^2 (Table 1), of all the 44 sets of data analyzed in this study;

Table 2
Fitted parameters of Eq. (8), (13), or (6), and related data for Clermont silt loam in the field under grass cover

Plot no.	Initial moisture	K (cm/h)	t_0 (min)	t_1 (min)	C	z_1 (mm)	Residual mean square (10^{-2} mm^2)	r (cm/h)
1	Dry	0.42	0.728	5.444	0.3588	3.90	3.43	8.3310
	Wet	0.95	2.624	2.624	0.3458	0.00	4.26	8.7378
2	Dry	0.89	1.938	6.122	0.3471	2.50	3.57	8.7378
	Wet	1.38	1.316	5.285	0.3378	2.62	7.88	9.0168
3	Dry	0.34	5.026	6.833	0.3620	0.42	11.59	8.4582
	Wet	1.83	1.948	4.204	0.3292	0.90	5.22	8.4792
4	Dry	1.55	0.896	4.954	0.3336	2.73	18.11	8.4582
	Wet	3.44	0.000	2.636	0.3146	2.64	11.10	9.4536
5	Dry	1.39	0.707	3.870	0.3390	2.50	8.71	9.5502
	Wet	0.34	0.772	3.756	0.3628	2.28	7.68	8.7378
6	Dry	1.11	0.260	3.953	0.3420	3.44	14.16	8.7378
	Wet	1.55	0.176	2.921	0.3364	2.73	6.12	9.5502
7	Dry	0.23	0.595	3.269	0.3678	2.16	16.12	8.7378
	Wet	0.96	0.023	4.127	0.3452	4.87	24.51	8.7378
Mean	Dry	0.85	–	–	–	2.52	–	–
Mean	Wet	1.49	–	–	–	2.29	–	–

Table 3
Fitted parameters of Eq. (8), (13), or (6), and related data for Chelsea sandy loam in the field

Plot no.	Initial moisture	K (cm/h)	t_0 (min)	t_1 (min)	C	z_1 (mm)	Residual mean square (10^{-2} mm^2)	r (cm/h)
With grass cover								
1	Dry	6.52	6.341	9.849	0.3090	1.23	3.75	14.908
	Wet	4.42	1.448	7.534	0.3172	5.29	2.91	13.396
2	Dry	5.55	12.734	16.381	0.3020	0.48	0.75	10.308
	Wet	3.81	2.383	7.143	0.3236	3.79	1.70	14.274
3	Dry	5.42	2.957	7.638	0.3146	3.12	0.78	14.929
	Wet	3.76	2.976	7.301	0.3238	3.05	0.53	14.285
4	Dry	5.61	4.322	8.608	0.3106	1.99	2.37	13.718
	Wet	4.47	3.435	8.925	0.3160	3.28	2.93	12.950
Mean	Dry	5.78	–	–	–	1.70	–	–
Mean	Wet	4.12	–	–	–	3.85	–	–
With fiberglass cover								
1	Dry	2.02	2.058	4.191	0.3390	1.41	0.77	13.779
	Wet	1.31	0.891	2.941	0.3480	1.97	1.17	13.614
2	Dry	3.69	3.766	3.766	0.3236	0.00	2.22	13.988
	Wet	2.18	2.548	3.246	0.3370	0.20	1.23	13.816
Mean	Dry	2.86	–	–	–	0.70	–	–
Mean	Wet	1.74	–	–	–	1.08	–	–

namely, the wet run of Plot 6 on Cincinnati silt loam as shown graphically in Fig. 2. Even so, the experimental points of w versus U fall relatively well upon the straight line through the origin

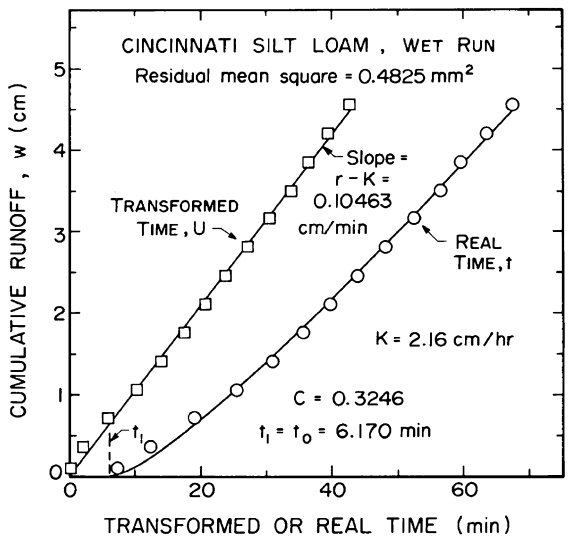

Fig. 2. Experimental points and fitted curves of cumulative runoff versus both transformed time (left curve, Eq. (15)) and real time (right curve, Eq. (13)), for the wet run on Plot 6 of Cincinnati silt loam.

(proportionality), in accordance with Eq. (15). The same good conformity obtains for the real-time points of w versus t in accordance with Eq. (13) in its curvilinearity. Hence, all of the remaining 43 data sets will display even better goodness of fit than in Fig. 2, because of their smaller RMS values. This can be seen for the dry run of the same Plot 6 on Cincinnati soil as shown in Fig. 3, in which the points of w versus T fall very well upon the linear curve of Eq. (12), as do the real-time points of w versus t in accordance with Eq. (8) in its distinctly curvilinear manifestation.

For the largest RMS of Clermont silt loam, the 0.2451 mm^2 (Table 2) from the wet run on Plot 7, the points of w versus T shown in Fig. 4 conform very well to the linear curve of Eq. (12), as do the points for the dry run on the same plot. The corresponding curves in real time for the dry and wet runs (Plot 7), shown in Fig. 5, also display excellent conformity with Eq. (8), although the curvilinearity is very slight. This does, however, demonstrate the versatility of Eq. (8), in accommodating near-linearity as well as curvature. Again, all of the remaining 13 data sets for Clermont soil will display better goodness of fit than

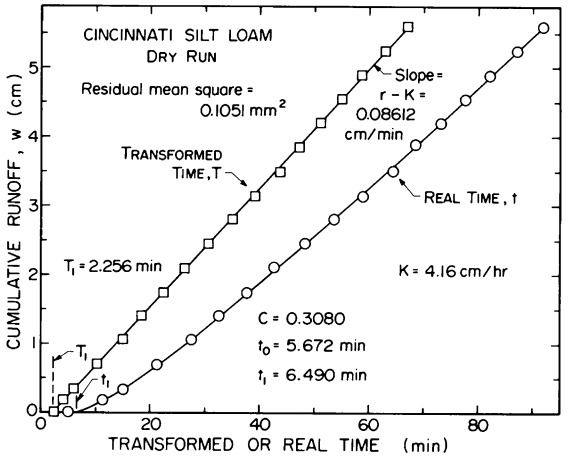

Fig. 3. Experimental points and fitted curves of cumulative runoff versus both transformed time (left curve, Eq. (12)) and real time (right curve, Eq. (8)), for the dry run on Plot 6 of Cincinnati silt loam.

the wet run of Fig. 4, because of their smaller RMS values.

Finally, for the largest RMS of Chelsea sandy loam, the 0.0375 mm^2 (Table 3) from the dry run on Plot 1 is only about 8% of that for the Cincinnati silt loam in Fig. 2. Therefore, each point in Fig. 6 for the dry run and in Fig. 7 for the wet run falls almost perfectly on its fitted curve, whether from the transformed-time Eq. (12) or the real-time Eq. (8). Once more, because their RMS values are smaller, all

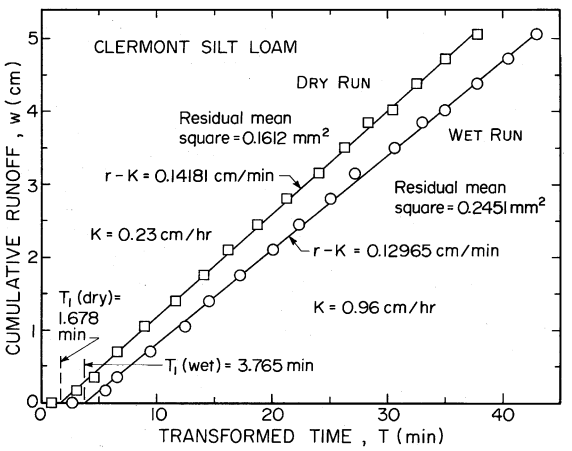

Fig. 4. Experimental points and fitted curves (Eq. (12)) of cumulative runoff versus transformed time for the dry and wet runs on Plot 7 of Clermont silt loam.

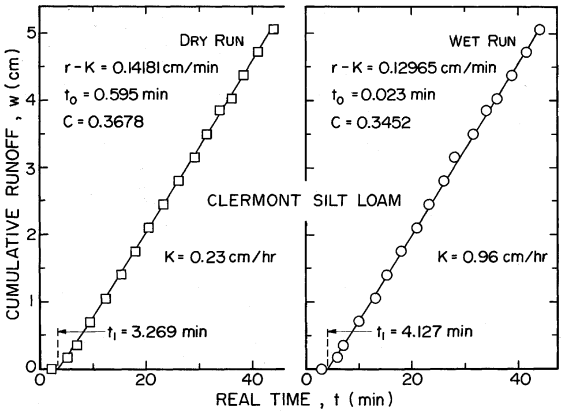

Fig. 5. Experimental points and fitted curves (Eq. (8)) of cumulative runoff versus real time for the dry and wet runs on Plot 7 of Clermont silt loam.

of the remaining 11 data sets for Chelsea soil will exhibit better goodness of fit than Fig. 6.

4.2. Sated hydraulic conductivity K

Using the split-plot design to analyze the K values statistically for all soils and cover, all main effects and interactions were statistically significant at least at the 5% level, and LSD values were calculated for

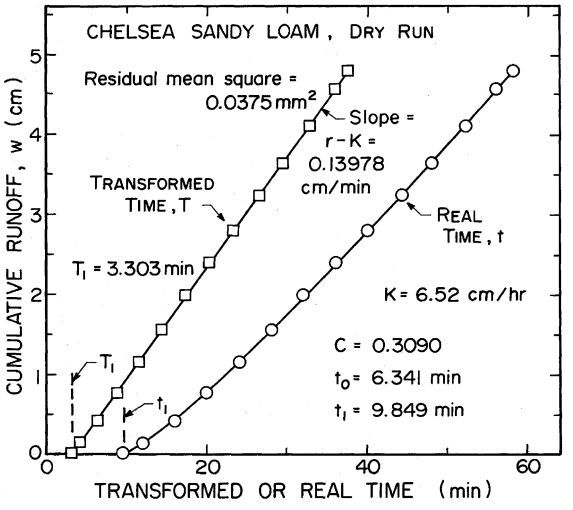

Fig. 6. Experimental points and fitted curves of cumulative runoff versus both transformed time (left curve, Eq. (12)) and real time (right curve, Eq. (8)), for the dry run on Plot 1 of Chelsea sandy loam with grass cover.

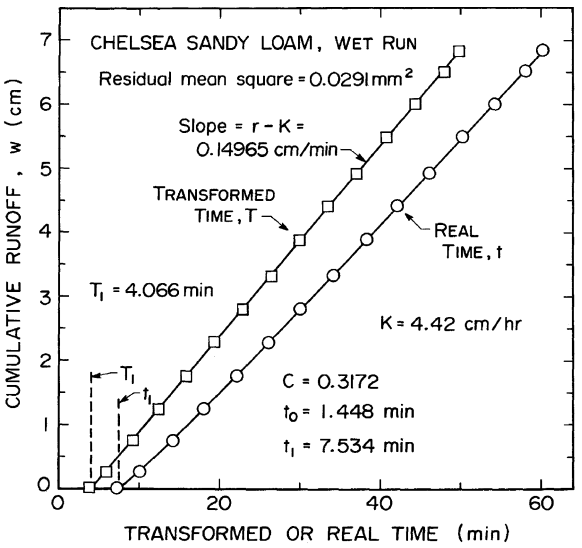

Fig. 7. Experimental points and fitted curves of cumulative runoff versus both transformed time (left curve, Eq. (12)) and real time (right curve, Eq. (8)), for the wet run on Plot 1 of Chelsea sandy loam with grass cover.

the mean values of K within soils-cover. For Cincinnati and Chelsea soils, as shown in the upper half of Table 4, the mean K values within soils-cover for the wet runs were lower than for the dry runs, but the reduction was statistically significant only for Chelsea-grass (1% level). For Clermont-grass, the increase in mean K for the wet runs was significant at the 5% level.

Of further interest was the extent to which the mean K values could detect and measure differences between soils and cover within wet or dry. Within the dry runs, Cincinnati-grass and Chelsea-fiberglass could not be separated from each other statistically with Duncan's test at the 5% level, as indicated in Table 4 by the connective underline of the mean K values 2.26 and 2.86 cm/h. This intermediate grouping could, however, be separated at the 5% level from the Clermont-grass below and the Chelsea-grass above, as indicated in Table 4 by the absence of connective underlining of the mean K values 0.85 and 5.78 cm/h. Similar examination of the mean K values within the wet runs shows that the Clermont-grass, Cincinnati-grass, and Chelsea-fiberglass could not be separated from each other, but this 3-member grouping was significantly different statistically (5% level) from the higher value for Chelsea-grass.

4.3. Static surface storage z_1

The z_1 values for each plot and run, calculated from Eq. (6), were also analyzed by the split-plot statistical design for all soils and cover. Only the main effect was statistically significant at the 5% level, and LSD values were calculated for the mean values of z_1 within soils-cover. As shown in the lower half of Table 4, differences in wet versus dry within

Table 4
Comparison of mean sated hydraulic conductivity K, and of mean static surface storage z_1, within soils-cover (least significant differences, LSD), and within initial soil moisture, dry or wet runs (Duncan's test, 5% level)

Initial moisture	Clermont-grass (cm/h)	Cincinnati-grass (cm/h)	Chelsea-fiberglass (cm/h)	Chelsea-grass (cm/h)
K (dry)	0.85	2.26	2.86	5.78
K (wet)	1.49	1.89	1.74	4.12
K (wet) − K (dry)	0.64	−0.37	−1.12	−1.66
LSD, 5%	0.61	0.54	1.14	0.81
LSD, 1%	0.84	0.74	1.57	1.11

	Cincinnati-grass (mm)	Chelsea-fiberglass (mm)	Chelsea-grass (mm)	Clermont-grass (mm)
z_1 (dry)	0.34	0.70	1.70	2.52
z_1 (wet)	0.28	1.08	3.85	2.29
z_1 (wet) − z_1 (dry)	−0.06	0.38	2.15	−0.23
LSD, 5%	1.00	2.13	1.50	1.14
Number of observations in each dry or wet	7	9	2	4	7

soils-cover were generally not statistically significant at the 5% level, except for the higher wet value of Chelsea-grass. Comparing the means for soils-cover by Duncan's test within dry or wet, as expressed by interruptions in underlining (Table 4, lower half), then clearly the small values for Cincinnati-grass were always significantly smaller than those for Chelsea-grass (broken underline) and Clermont-grass, even though these last two were not always significantly different from each other (dry run, connective underline of z_1 values 1.70 and 2.52 mm). This is consistent with the steeper plot slope (5%) of the Cincinnati-grass in comparison with that of the Chelsea-grass (0%) and the Clermont-grass (0.5%).

5. Discussion and conclusions

From Figs. 2–7, it is demonstrated conclusively that Eq. (8) or (13) is an excellent representation of the infiltrometer runoff curves for 44 sets of data on three different soils. Also, for the same cover (grass), K tends toward the soils sequence Chelsea > Cincinnati > Clermont, which is relatively consistent with the decreasing particle sizes in these soils.

In another respect, however, the K behavior seems less acceptable. Presumably, since K purports to be the sated (near-saturated) conductivity, its value should be the same for both the dry and wet runs. But for the Cincinnati and Chelsea soils, K is smaller for the wet runs. Physically, this could happen if the sprinkled water entraps more air in the initially wetter soils, or if the soil structural arrangement is somehow degraded by the first sprinkling of water. In contrast, the Clermont soil exhibits a statistically significant increase of K from the dry run to the wet. We note that at about 75 cm below the surface of this soil there is a less permeable layer, which arguably might have caused the surface soil zone to remain relatively wet after the first sprinkling of water. Some of the entrapped air might then have dissolved in the soil water prior to the second sprinkling, thus causing K to increase. Unfortunately, experimental assessment of this explanation is not possible, because field measurements of initial soil water content before both dry and wet runs were reported for the Cincinnati soil (mass-basis 19.1 and 26.8% for dry and wet runs, respectively), but not for the Clermont or Chelsea.

The behavior of the Clermont K might also mean that the present theory, embodied in Eqs. (8) and (13) and ultimately matched to the idealized Green–Ampt model, is inadequate for the Clermont soil but is more adequate for a sandy soil (Philip, 1957, p. 261) such as the Chelsea. Hence, the present theory may need some generalizing revision, despite its success in the sense of Figs. 2–7 (especially Figs. 6 and 7 for Chelsea). We note also that the measurements of the Clermont K have suffered in accuracy from using values of r that turn out to be somewhat too large relative to K. This then produces a slope $(r - K)$ of the transformed fitting line (Fig. 4) that approaches r in magnitude, so that K is evaluated as a small difference between two relatively large numbers. Again, the values of K/r for Chelsea were much more favorable (larger) than for Clermont. It would be desirable for K/r to be in the range 0.5–0.8 if possible.

With the static surface storage z_1 being distinctly smaller for the steeper slope, and tending to be larger for grass than for fiberglass, these reasonable physical and statistical responses thus support the simplified storage concept used in arriving at Eqs. (6), (8), and (13). Nonetheless, in any attempted revision of theory, it would still seem worthwhile to attempt to supplement the static z_1 with at least a simplified transient surface storage component, sometimes called detention.

On balance, the proposed method of measuring K with a small sprinkling infiltrometer is promising. K values for surface soils are enabled, which have been difficult to obtain by other methods. Refinements in theory and experimental practice should have the potential to circumvent the shortcomings that have been noted here.

Acknowledgements

Contribution from the Department of Agronomy, Purdue University Agricultural Research Programs, West Lafayette, IN 47907, USA, Journal Paper No. 16,738; the Department of Agronomy and Horticulture, University of Nebraska Agricultural Research Division, Lincoln, NE 68583, USA, Journal Series

No. 13,594; and the Al-Fatah University, Tripoli, Libya. We thank Dr Eileen J. Kladivko, Professor, Purdue University, for manuscript review and administrative processing assistance; Dr R.P. Ewing, Professor, Iowa State University, for manuscript review; and, from the Department of Agronomy and Horticulture, University of Nebraska-Lincoln, Bette L. Schernikau, Project Assistant, for word processing of the manuscript, and Wallace W. Troyer, Research Technologist, for assistance with the figures.

References

Amerman, C.R., Hillel, D., Peterson, A.E., 1970. A variable-intensity sprinkling infiltrometer. Soil Sci. Soc. Am. Proc. 34, 830–832.

Bertrand, A.R., Parr, J.F., 1961a. Development of a portable sprinkling infiltrometer. Int. Congr. Soil Sci. Trans. Seventh (Madison, WI, USA), 1960 I, 433–440.

Bertrand, A.R., Parr, J.F., 1961b. Design and operation of the Purdue sprinkling infiltrometer. Purdue Univ. Agric. Exp. Stn. Res. Bull. 723, 16.

Gilman, R.D., 1962. Infiltration measurements under different management practices. MS Thesis, Purdue University, West Lafayette, IN, USA.

Green, W.H., Ampt, G.A., 1911. Studies on soil physics. I. Flow of air and water through soils. J. Agric. Sci. (Cambridge) 4, 1–24.

Lambert, R.L., 1970. The testing of a method for predicting water intake into soils by the use of field cores. PhD Thesis, Purdue University, West Lafayette, IN, USA.

Miller, R.D., Bresler, E., 1977. A quick method for estimating soil water diffusivity functions. Soil Sci. Soc. Am. J. 41, 1020–1022.

Philip, J.R., 1957. The theory of infiltration. 4. Sorptivity and algebraic infiltration equations. Soil Sci. 84, 257–264.

Rawitz, E., Margolin, M., Hillel, D., 1972. An improved variable-intensity sprinkling infiltrometer. Soil Sci. Soc. Am. Proc. 36, 533–535.

Swartzendruber, D., 1974. Infiltration of constant-flux rainfall into soil as analyzed by the approach of Green and Ampt. Soil Sci. 117, 272–281.